Available online at www.sciencedirect.com
SCIENCE DIRECT®
Journal of Photochemistry and Photobiology A: Chemistry 170 (2005) 279–285
Journal of Photochemistry and Photobiology A:Chemistry
www.elsevier.com/locate/jphotochem

The effect of lanthanide on the degradation of RB in nanocrystalline Ln/TiO_2 aqueous solution

Yuhong Zhang*, Hailiang Xu, Yongxi Xu, Huaxing Zhang, Yanguang Wang

Department of Chemistry, Zhejiang University, Hangzhou 310027, China

Received 8 April 2004; received in revised form 31 August 2004; accepted 1 September 2004
Available online 8 October 2004

Abstract

A series of Nd^{3+}, Pr^{3+}, Er^{3+}, and Dy^{3+} (0.25–5 at.%) homogeneously doped nanocrystalline titanium dioxides (Ln/TiO_2) were prepared by an easy sol–gel technique, and the roles of lanthanide doping on the photocatalytic activity in the degradation of rhodamine B (RB) in aqueous solution were studied. Both the concentration of the lanthanide dopant and calcination temperature showed significant effect to the photodegradation of RB. The photocatalytic activity of pure titania was drastically decreased when calcination temperature was at 700 °C, while the high photocatalytic activity was still maintained for lanthanide-doped samples. HPLC-MS method was used to study the degradation process, and it is demonstrated that the degradation of RB catalyzed by Ln/TiO_2 was principally go through with a stepwise de-ethylation photochemical process.

Keywords: Ln/TiO_2; Degradation; Rhodamine B

1. Introduction

One of the major sources of environmental contaminations is dyestuff which mainly comes from the textile and photographic industries [1–3]. The conventional methods such as flocculation, osmosis, and activated carbon absorption showed a limited efficiency for the treatment of dye-containing wastewaters due to the increased refractory pollutants in the effluents and expensiveness. The advanced oxidation technologies, such as TiO_2-mediated photocatalysis, have been extensively investigated for the destruction of dye pollutants in the past few years [4–6].

TiO_2 has three natural phase modifications: brookite, anatase, and rutile. Anatase is commonly believed to be the active phase [7]. Ultrafine TiO_2 powders have larger specific surface areas and are expected to have good catalytic activities since reactions take place on the TiO_2 surface [8]. However, the pure ultrafine TiO_2 powders often agglomerate into larger particles, which resulted in an adverse effect on the catalytic performance. Doping different valence metal ions into TiO_2 is proven to be able to alter both the photoactivity and A–R (anatase-to-rutile) phase transformation of titania [9–20]. Recently, others and we reported the lanthanide-doped TiO_2 [20–31]. Lanthanide ions are known for their ability to form complexes with various Lewis bases (e.g., amines, aldehydes, thiols, etc.) in the interaction of these functional groups with the f-orbitals of the lanthanides. Thus, incorporation of lanthanide ions in a TiO_2 matrix could provide a means to concentrate the organic pollutant at the semiconductor surface and therefore enhance the photoactivity of titania. We found that the performance of the europium-doped titania was dependent on the preparation procedure, the distribution, and the concentration of europium ions [31]. In this paper, we describe the preparation of a series of lanthanide homogeneously doped nanosized TiO_2 and their photocatalytic properties for degradation of RB in aqueous solution.

* Corresponding author. Tel.: +86 571 87953253; fax: +86 571 87951895.
E-mail address: yhzhang@zjuem.zju.edu.cn (Y. Zhang).

1010-6030/$ – see front matter © 2004 Elsevier B.V. All rights reserved.
doi:10.1016/j.jphotochem.2004.09.001

The results indicated that the activity of TiO_2 was significantly improved by lanthanide doping, and the degradation process catalyzed by Ln/TiO_2 carried out with a stepwise process.

2. Experimental

2.1. Preparation of samples

Neodymium (NT), praseodymium (PT), dysprosium (DT), and erbium (ET) homogeneously doped titania were prepared by an easy sol–gel technique, which has been reported elsewhere [18]. A typical procedure for the preparation of lanthanide-doped titania is given below: the required stoichiometric oxide lanthanide (99.9%, ACROS) was dissolved in a minimum amount of nitric acid and evaporated to dryness. The dry lanthanum nitrate was dissolved in butanediol (2 g), and tetrabutyl-orthotitanate (98%, ACROS, 3 g) was added into the solution at room temperature by stirring. A homogeneous transparent solution was formed. The solution was very stable and no changes took place for more than 1 year when it is preserved in the sealed bottle. When the solution was exposed in air at room temperature for 1 week, a dry solid gel resulted, which is further heated at 120 °C for 5 h. The doped nanocrystalline was finally obtained by heating the dry solid gel at different temperatures above 400 °C for 1 h in air by using a Naber 7H furnace. The heating program is 3 °C/min for each sample. The samples containing 0, 0.25, 0.5, 1, 2, 3, and 5 at.% (mole percentage) neodymium are labeled as NT0, NT1, NT2, NT3, NT4, NT5, and NT6. The samples containing 0, 0.25, 0.5, 1, 2, 3, and 5 at.% dysprosium are labeled as DT0, DT1, DT2, DT3, DT4, DT5, and DT6. Identical concentration of Pr- and Er-doped samples were prepared and named analogously.

2.2. Photocatalysis measurements

The rhodamine B dye was of laser grade. Deionized water was used throughout the experiment. The photoactivity of as-prepared samples is detected by the degradation of rhodamine B at ambient temperature. The aqueous RB/Ln–TiO_2 dispersions were prepared by the addition of Ln–TiO_2 (50 mg) to a 25-mL aqueous solution containing RB dye ($C_0 = 10^{-5}$ M). Prior to the irradiation, the suspensions were stirred for 15 min to ensure the establishment of suitable adsorption/desorption equilibrium of the dye on the surface of Ln/TiO_2 or TiO_2. A 300 W 365 nm UV lamp (Institute of Electric Light Source, Shanghai, China) was surrounded by a circulating water jacket (Pyrex) to cool the lamp. The distance between UV lamp and reactor is 30 cm for each experiment. After irradiation and removal of the Ln–TiO_2 particles by centrifugation and filtration, the filtrates were analyzed by a Shimadzu UV-2000 spectrophotometer.

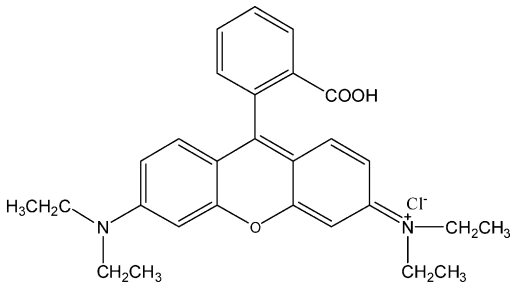

Rhodamine-B

2.3. Characterization

The analysis of the original dye and *N*-de-ethylated intermediates was performed on an HPLC-MS equipment (Agillent-1100, Bruker Esquire 3000t) using an YMC C-18 column under normal-phase condition. The mobile phase was a methanol/water gradient ranged from 60 to 90% at a flow rate of 0.8 mL min^{-1}. HPLC grade methanol and HPLC grade water were used throughout the analysis. The crystal and the structure/modification of the products were studied on a Bruker D8 X-ray diffractometer using Cu Kα radiation. The identification of crystalline phases was accomplished by comparison with JCPDS files numbered as 21-1272, 21-1276, 33-943, 45-265, 17-453, and 18-499 for anatase, rutile, neodymium titanium oxide ($Nd_4Ti_9O_{24}$), praseodymium titanium oxide ($Pr_4Ti_9O_{24}$), dysprosium titanium oxide ($Dy_2Ti_2O_7$), and erbium titanium oxide ($Er_2Ti_2O_7$), respectively. The average crystal size was determined from the anatase peak broadening (1 0 1) crystal plane for anatase with Scherrer's equation.

3. Results and discussion

3.1. Characterization of lanthanide-doped titania

The phase transformation of lanthanide-doped TiO_2 depends on the dopants and their concentration. Fig. 1 presents

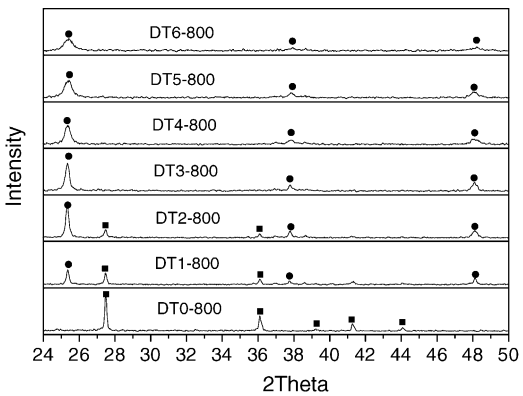

Fig. 1. XRD diffraction patterns of dysprosium-doped titania samples calcined at 800 °C for 1 h in air: (■) rutile; (●) anatase.

the XRD results of dysprosium-doped titania calcined at 800 °C for 1 h in air. The transformation of anatase-to-rutile of pure as-prepared nanosized TiO_2 took place between 630 and 700 °C. Thus the pure as-prepared TiO_2 only shows a single rutile phase in Fig. 1. It should be noted that a mixture of anatase and rutile is still maintained in 0.25% dysprosium-doped sample calcined at 800 °C. When the concentration of dysprosium is increased to 0.5 at.%, the relative intensity of rutile is decreased remarkably. Further increasing of the dysprosium content to 1 at.%, a single anatase phase is observed, demonstrating that dysprosium doping has a significant inhibitory effect to the A–R phase transformation. It is manifest that this remarkable shift of the phase transformation to high temperatures is caused by the lanthanide doping. It is expected that the surrounding lanthanide ions will inhibit the phase transition of anatase-to-rutile through the formation of Ti–O–Ln bond. On the other hand, the Ln_2O_3 lattice locks the Ti–O species at the interface with the TiO_2 domains preventing the nucleation that is necessary for anatase transformation to rutile.

There is an optimal dopant concentration in which the observed inhibitory effect achieves the maximum. Fig. 2 presents the XRD reflections of dysprosium-doped titania calcined at 900 °C. It can be seen that 0.25 and 0.5% doped samples show a mixture phase of anatase and rutile, and the relative ratio of rutile/anatase is reduced with increasing lanthanide content. Further increasing lanthanide content to 1%, only a small rutile reflection was observed and a main anatase phase was retained. It is interesting to note that the relative ratio of rutile/anatase was increased when the lanthanide content enhanced to 3% (LT5), inferring a reduction of A–R phase transition temperature. In 5% doped samples, the rutile became the main phase. It is evident that the optimum inhibitory effect is the 1–2% lanthanide-doped sample. The precise mechanism for this change is unclear but may be related to the formation of lanthanide titanium oxides ($Dy_2Ti_2O_7$) and enhancement of defects for high lanthanide content samples. Likely, the number of defects inside the anatase phase is grown with the enhancement of lanthanide oxide, and the defects in excess may be favorable to the formation and growth of rutile nuclei [32]. Lanthanide titanium oxide is appeared at high heating temperatures. The evolution temperatures for lanthanide titanium oxide are progressively reduced with the enhancement of lanthanide concentration. It is not easy to obtain a conclusion about a link between A–R transformation and the formation of lanthanide titanium oxide, but the easy formation of lanthanum titanium oxide for high lanthanum content titania samples may catalyze the mass transport to the nucleation region of rutile phase, promoting rutile nuclei growth, and therefore favoring the phase transformation. XRD reflections belonging to lanthanide oxide(s) are not found in all as-prepared samples. These findings are consistent with the results of transition metal ion-doped titania prepared by this technique [18], implying that lanthanide is better dispersed in TiO_2 matrix. The oxide lanthanides reflections were observed where the aqueous nitric acid solution was applied for the preparation of rare-earth-doped titania during the sol–gel process [26].

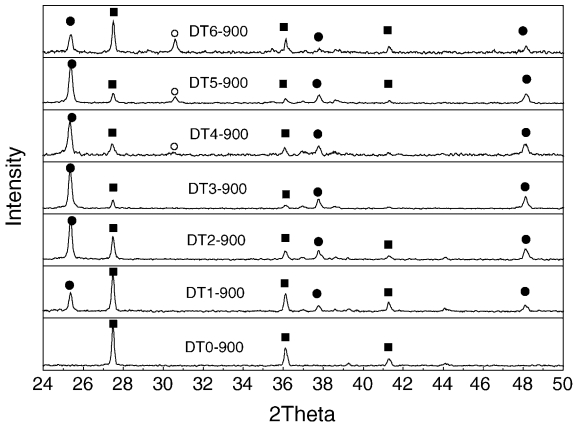

Fig. 2. XRD diffraction patterns of dysprosium-doped titania samples calcined at 900 °C for 1 h in air: (■) rutile; (●) anatase; (◯) dysprosium titanium oxide ($Dy_2Ti_2O_7$).

The effect of other lanthanide on the A–R phase transformation of TiO_2 is similar to dysprosium doping. Table 1 presents the phase transformation results of 3 at.% various lanthanide-doped TiO_2. It is demonstrated that the all 3% lanthanide-doped samples only show an anatase phase when calcined at 800 °C for 1 h in air, showing very strong inhibitory efficient to the A–R phase transformation. After these samples were heated at 900 °C for 1 h in air, the rutile reflections were emerged in the XRD pattern, and at the same time, the lanthanide titanium oxides were formed ($Pr_4Ti_9O_{24}$, $Nd_4Ti_9O_{24}$, $Dy_2Ti_2O_7$, $Er_2Ti_2O_7$). Larger radius lanthanides prefer to form higher coordination number lanthanide titanium oxide.

From the broadness of the anatase peak (1 0 1), the average crystallite sizes of the lanthanide-doped titania calcined 700 °C for 1 h in air were calculated (Table 2) by Scherrer's equation. Obviously, the lanthanide-doped samples have finer crystallites than undoped titania. The average crystallite size was 56 nm calcined at 700 °C for undoped titania, while a considerable reduction in size was observed after doping with 1% lanthanides. With the increase of lanthanide dopant content, the average crystallite size progressively decreased. This reduction in crystallite size is proposed to be

Table 1
The phase modification of 3 at.% lanthanide-doped titania calcined at different temperatures

Temperature (°C)	Sample				
	PT5	NT5	ET5	DT5	Pure TiO_2
500–630	A	A	A	A	A
640–700	A	A	A	A	A, R
710–800	A	A	A	A	R
900	A, R, PTO	A, R, NTO	A, R, HTO	A, R, DTO	R

A: anatase; R: rutile; PTO: $Pr_4Ti_9O_{24}$; NTO: $Nd_4Ti_9O_{24}$; ETO: $Er_2Ti_2O_7$; DTO: $Dy_2Ti_2O_7$.

Table 2
Average grain size of the neodymium- (NT), praseodymium- (PT), dysprosium- (DT), and erbium- (ET) doped titania calcined at 700 °C for 1 h in air calculated by Scherrer's equation

	Grain size at lanthanide content (at.%)						
	0	0.25	0.5	1	2	3	5
NT–700 (nm)	56	27	23	16	11	11	9
PT–700 (nm)	56	28	23	22	13	11	10
DT–700 (nm)	56	33	25	20	13	11	12
ET–700 (nm)	56	29	23	16	12	11	10

due to segregation of the dopant cations at the grain boundary, which inhibits the grain growth by restricting direct contact of grains [32].

3.2. Photodegradation of RB

The degradation of RB was investigated by using the as-prepared catalysts under UV irradiation (380–450 nm). The UV–vis spectra variations of RB aqueous solution catalyzed by pure TiO_2 and Nd/TiO_2 (NT4, neodymium 2 at.%) under different irradiation times are displayed in Fig. 3. The aqueous solution of tetra-ethylated rhodamine (RB, 10^{-5} M) shows a major absorption band at 552 nm in the absence

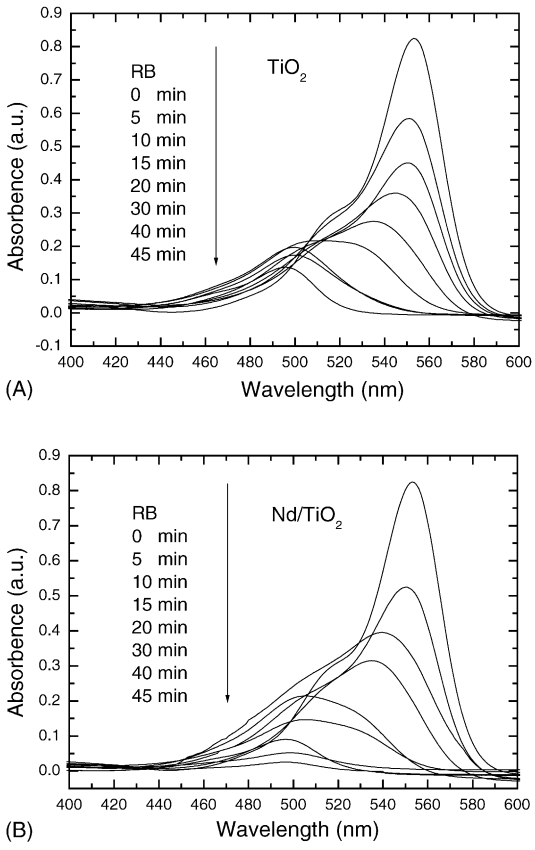

Fig. 3. UV–vis spectral changes of RB as a function of irradiation time. Spectrum RB is the UV–vis spectrum of RB (10^{-5} M, pH = 7) before addition of TiO_2 or Ln/TiO_2 particles to the solution. Absorbance changes catalyzed by (A) TiO_2 and (B) Nd/TiO_2. TiO_2 and Nd/TiO_2 (NT4, 2 at.%) were calcined at 500 °C for 1 h in air.

of TiO_2 or Ln/TiO_2. The absorbencies of the dispersion of RB/TiO_2 or RB/Ln–TiO_2 were decreased obviously after the magnetic stirring for 30 min in the dark, reflecting the extent of adsorption of RB on catalysts. It should be noted that the absorbance reduction of RB/TiO_2 is smaller than that of RB/Ln–TiO_2, inferring that more RB molecules were adsorbed on Ln/TiO_2. Lanthanide ions are proven to have the ability to form complexes with various Lewis bases in the interaction of these functional groups [33]. It is evident that the lanthanide dopants in a TiO_2 matrix provide the means to concentrate the RB at Ln–TiO_2 surface with coordination and leads to the more decreasing of absorbance. In addition, the smaller particle size of doped samples induced by lanthanide doping should play the role to the absorbance reduction as well.

Both de-ethylation and degradation of RB chromophore structure may take place in the presence of photocatalysts under UV irradiation. In fact the degradation of RB chromophore structure and de-ethylation are two competitive reactions during the RB photodegradation. The de-ethylation of the fully *N*,*N*,*N*′,*N*′-tetraethylated rhodamine molecule has the wavelength position of its major absorption band moved toward the blue region (RB, 552 nm; *N*,*N*,*N*′-tri-ethylated rhodamine, 539 nm; *N*,*N*′-di-ethylated rhodamine, 522 nm; *N*-ethylated rhodamine, 510 nm; and rhodamine, 498 nm) [33]. According to the studies of Watanabe et al. [34–35], •OH radicals in the solution bulk attack principally at the aromatic chromophore ring, leading to the degradation of RB structure and the reduction of absorption without wavelength shift. By contrast, the de-ethylation is mainly a surface occurring reaction, causing the significant blue wavelength shifts. The temporal spectral changes of the photodegradation of RB mediated by TiO_2 (Fig. 3A) showed that the absorption was decreased with the concomitant small wavelength shift of band to the shorter wavelengths after the irradiation of 15 min. These observations indicate that in the dispersion of TiO_2, both the cleavage of RB aromatic chromophore ring structure and the de-ethylation take place, with the predominating RB structure degradation during the initial irradiation period. However, the hypsochromic shifts of the absorption maximum in Ln/TiO_2 dispersion was pronounced (Fig. 3B) throughout the irradiation. It is seen that after the irradiation of 5 min, the maximum absorbance of band moved from 552 to 540 nm. The maximum absorption was rapidly shifted to 504 nm after 15 min (Table 3). Further irradiation caused the band moved to 498 nm, indicating that the full de-ethylated product was achieved. Clearly, the RB photodegradation in

Table 3
Wavelength shift in absorption maximum (nm) with different irradiation time catalyzed by pure TiO_2 and NT4 (2 at.%) calcined at 500 °C for 1 h in air

	Wavelength shift at time (min)						
	0	5	10	15	20	25	30
TiO_2 (500 °C)	554	554	545	536	515	515	501
NT4 (500 °C)	554	541	535	505	505	505	501

the Ln/TiO_2 dispersion is mainly the de-ethylation by a stepwise manner.

To get a better handle on the RB degradation details of lanthanide-doped titania, HPLC-MS method was used to examine the temporal intermediates occurring in the RB solution. The aqueous solution separated from the photocatalyst (NT4, Fig. 3B) after irradiating at different time was extracted by ethyl acetate solvent and analyzed by HPLC-MS technique. The results of HPLC were presented in Fig. 4 and six chromatographic bands were clearly evidenced. Except for the RB dye (peak A), the peaks increased first and subsequently decreased, indicating the formation and transformation of the intermediates. The relevant mass spectrograms are illustrated in Table 4. The five intermediates were identified to be the intermediate products having the different number of *N*-methyl group. It is concluded from the related mass spectrograms (Table 4) that peak B corresponds to the intermediate losing one ethyl group. Peaks C and D are ascribed to the intermediates possessing two less ethyl groups and correlate with two isomeric molecules. One isomer is formed by removal of one ethyl group from each side of the RB molecule, and the other isomer is produced by removal of two ethyl groups from same side. Both intermediates display the identical mass spectra data. Peak E is produced by removal of three ethyl groups from the RB molecule and the full de-ethylated product corresponding to peak F is formed. The successive appearance of the maximal quantity of each intermediate further confirms that the degradation of the RB catalyzed by lanthanide-doped TiO_2 under the UV irradiation is a stepwise photochemical process.

The detailed mechanism of titania-photocatalyzed reactions is differed from one substrate to another. However, it is widely recognized that the superoxide, and in particular, the hydroxy radical ($OH^{\bullet}$), act as the active agents to the mineralization of the organic compounds. The radicals produced by irradiation of UV light on the titania particles is shown below:

$$O_2 + e_{CB}{}^- \rightarrow O_2{}^{\bullet -} \quad (1)$$

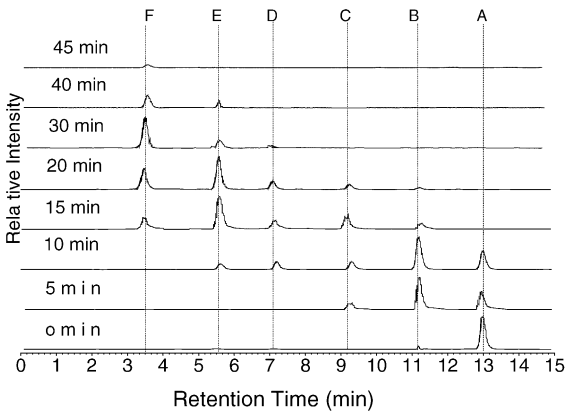

Fig. 4. HPLC chromatograms of the *N*-de-ethylated intermediates at different irradiation times. The corresponding UV–vis absorption was shown as Fig. 3B.

$$H_2O + h_{VB}{}^+ \rightarrow {}^{\bullet}OH + H^+ \quad (2)$$

$$^{\bullet}OH + {}^{\bullet}OH \rightarrow H_2O_2 \quad (3)$$

$$H_2O_2 + O_2{}^{\bullet -} \rightarrow {}^{\bullet}OH + OH^- + O_2 \quad (4)$$

The insertion of $^{\bullet}OH$ in the C–H bonds causes ultimately to the complete degradation of RB, while the attacking of $^{\bullet}OH$ at the *N*-ethyl group leads the de-ethylation [34,35]. Although the photocatalysis of titania is mainly a surface reaction and de-ethylation is the predominant reaction on the surface of titania, the cleavage of RB aromatic chromophore ring is also occurred in the solution bulk because of the existence of equilibrium of RB and its intermediates (RBn) between TiO_2 surface and solution bulk. Therefore both de-ethylation and structure degradation was observed in TiO_2 dispersion during the UV irradiation. Contrarily, in the RB/Ln–TiO_2 dispersion, the lanthanide ion in the TiO_2 matrix bonded the RB molecule at the surface by coordination, which halted the equilibrium of RB and its intermediates (RBn) between the TiO_2 surface and solution bulk and caused the degradation principally took place at the surface of titania. The remarkable wavelength shift toward shorter wavelengths in RB/Ln–TiO_2 dispersion was ascribed to the predominant de-ethylation reaction of the degradation, inferring that the lanthanide played an important role in the photodegradation process of RB.

Other lanthanide-doped titania samples exhibit the similar degradation process. Fig. 5 shows the dependence of photodegradation rate on the lanthanide concentration of Nd^{3+}-, Pr^{3+}-, Dy^{3+}-, and Er^{3+}-doped samples calcined at 500 °C for 1 h in air. It is seen that the photoactivity of lanthanide-doped TiO_2 is increased significantly comparing with the undoped titania and the highest photoactivity is generated by the 1 at.% lanthanide-doped samples. Further increase of lanthanide concentration induced a steady decrease of degradation rate, although the photoactivity of per individual lanthanide-doped TiO_2 was still higher than undoped TiO_2. From the point of coordination, high content lanthanide-doped samples should be favorable to the more complex formation, and thus the more RB molecules should be absorbed, and enhanced activity should be observed with higher lanthanide content titania samples. Our results, however, showed that the maximum photodegradation rate was produced by 1 at.% lanthanide-doped samples. Therefore, the concentration of substrate at the semiconductor surface by forming complex is likely not the only factor that influences the activity. Further studies are in progress to elucidate the mechanism.

The photoactivity of pure and lanthanide-doped TiO_2 heated at 700 °C for 1 h in air was shown in Fig. 6. The bare titania only displayed poor activity to the degradation of RB. In contrast to undoped titania, the degradation activity of all lanthanide-doped samples was markedly improved, and the higher the lanthanide concentration, the better the photoactivity. The reason for this remarkable activity improvement should be contributed to many factors. First, the lanthanide doping restrains the A–R phase transformation of the TiO_2. As shown in Table 1, all lanthanide-doped TiO_2

Table 4
Identification of RB and de-ethylation intermediates by HPLC-MS for RB/Ln–TiO_2 system

Absorption peak	Retention time (min)	De-ethylation intermediates	MS peak	Assigned substrates
A	13.0	*N*,*N*,*N*′,*N*′-Tetraethylrhodamine (RB)	443	RB–H
			465	RB–H–Na
B	11.1	*N*,*N*-Diethyl-*N*′-ethylrhodamine (TRB)	415	TRB–H
			437	TRB–H–Na
C	9.2	*N*-Ethyl-*N*′-ethylrhodamine (DRB)	387	DRB–H
			409	DRB–H–Na
D	7.1	*N*,*N*-Diethylrhodamine (DDRB)	387	DDRB–H
			409	DDRB–H–Na
E	5.5	*N*-Ethyl-rhodamine(MRB)	359	MRB–H
				MRB–H–Na
F	3.5	Rhodamine (RM)	331	RM–H
			353	RM–H–Na

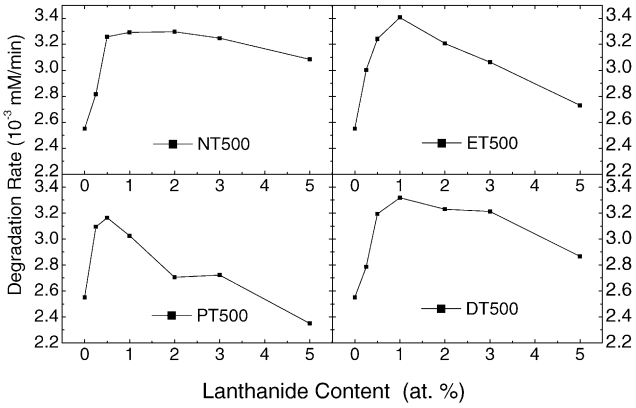

Fig. 5. The degradation rate of various lanthanide-doped titania with different content calcined at 500 °C for 1 h in air.

maintained the anatase phase after calcined at 700 °C for 1 h in air, but the A–R phase transformation of bare TiO_2 has almost finished. Therefore, the lanthanide-doped TiO_2 still preserved the anatase phase after the high-temperature calcinations, which shows the better performance than rutile in the photocatalysis. Second, as Ranjit et al. reported [28], the concentration of the RB at the surface of lanthanide-doped TiO_2 particles might be higher than that of bare titania particles because of the coordination of lanthanide with RB molecules. Finally, lanthanide doping has efficiently inhibited the agglomeration and sintering of TiO_2 at high temperatures and hence stabilized the nanosized titania (Table 2), which facilitated the photocatalysis as well. As we discussed earlier, the thermal stability effect of the lanthanide is proportional with the lanthanide concentration. High-concentration lanthanide samples show the smaller particle sizes, and therefore possess larger specific surface areas. Both of smaller particle size and larger surface area in lanthanide-doped TiO_2 were donated to the improvement of the photoactivity of Ln/TiO_2.

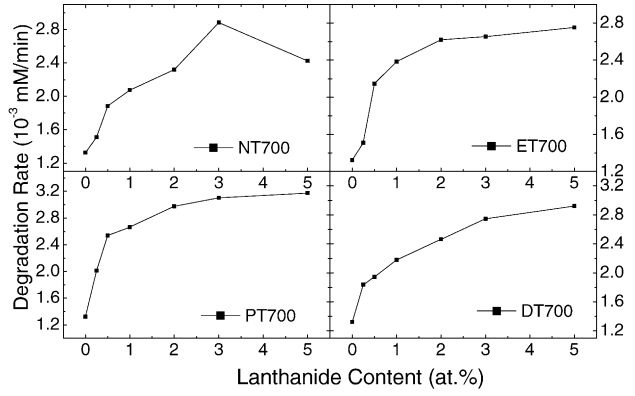

Fig. 6. The degradation rate of various lanthanide-doped titania with different content calcined at 700 °C for 1 h in air.

4. Conclusions

Titania samples with different amount of lanthanides were produced and their activity of photodegradation of RB was investigated. Comparing with pure TiO_2-, neodymium-, praseodymium-, dysprosium-, and erbium-doped titania exhibited much higher photoactivity. The concentrations of the lanthanide and calcination temperatures show the marked influences on the photoactivity of doped titania. It was worth to note that the good photoreactivity was still remained after the lanthanide-doped titania was heated at 700 °C for 1 h in air, which implicated a potential application of TiO_2 at high temperatures. The studies of RB degradation mechanism revealed that the lanthanide ions in TiO_2 matrix played important roles to the RB degradation process and the degradation of the RB catalyzed by lanthanide-doped TiO_2 under the UV irradiation was mainly a stepwise photochemical process.

Acknowledgments

Zhang acknowledges Prof. A. Reller for his discussions. This work was financed by Natural Science Foundation of China (No. 20373061) and Natural Science Foundation of Zhejiang Province, China (No. 202035).

References

[1] A. Fujishima, K. Hashimoto, T. Watanabe, TiO_2 Photocatalysis Fundamentals and Applications, BKC, Inc., Tokyo, 1999.
[2] W.C. Tincher, Text. Chem. Color. 21 (1989) 23.
[3] M.R. Hoffmann, S.T. Martin, W.Y. Choi, D.W. Bahnemann, Chem. Rev. 95 (1995) 69.
[4] K. Wu, Y. Xie, J. Zhao, H. Hidaka, J. Mol. Catal. 144 (1999) 77.
[5] B. O′Regan, M. Grätzel, Nature 353 (1991) 737.
[6] F. Herrera, J. Kiwi, A. Lopez, V. Nadtochenko, Environ. Sci. Technol. 33 (1999) 3145.
[7] R.J. Berry, M.R. Mueller, Microchem. J. 50 (1994) 28.
[8] J. Augustynski, Electrochim. J. 38 (1993) 43.
[9] D. Vorkapic, T. Matscukas, J. Am. Ceram. Soc. 81 (1998) 2815.
[10] H. Zhang, J.F. Banfield, J. Mater. Res. 15 (2000) 437.
[11] J. Soria, J.C. Conesa, V. Augugliaro, L. Palmisano, M. Schiavello, A. Sclafani, J. Phys. Chem. 95 (1991) 274.
[12] M.I. Litter, J.A. Navio, J. Photochem. Photobiol. A 98 (1996) 171.
[13] P.O. Larsson, A. Andersson, Appl. Catal. B 24 (2000) 175.
[14] K.E. Karakitsou, X.E. Verykios, J. Phys. Chem. 97 (1993) 1184.
[15] S.T. Martin, C.L. Morrison, M.R. Hoffmann, J. Phys. Chem. 98 (1994) 13695.
[16] H. Schneider, A. Baiker, V. Schar, A. Waukaun, J. Catal. 146 (1994) 545.
[17] J. Yang, J.M.F. Ferreira, Mater. Lett. 36 (1998) 320.
[18] (a) Y.H. Zang, A. Reller, J. Mater. Chem. 11 (2001) 2537;
(b) Y.H. Zhang, S. Ebbinghaus, A. Weidenkaff, A. Reller, T. Kurz, H.A.K. Nidda, P.J. Klar, M. Güngerich, Chem. Mater. 15 (2003) 4028;
(c) Y.H. Zhang, A. Reller, Mater. Lett. 57 (2003) 4108.
[19] W. Choi, A. Termin, M.R. Hoffmann, J. Phys. Chem. 98 (1994) 13669.
[20] R. Abe, K. Sayama, H. Arakawa, Chem. Phys. Lett. 371 (2003) 360.
[21] T. Lopez, J. Hernandez-Ventura, R. Gomez, F. Tzompantzi, E. Sanchez, X. Bokhimi, A. Garcýa, J. Mol. Catal. A: Chem. 167 (2001) 101.
[22] K.N.P. Kumar, A. Burggraaf, J. Mater. Chem. 3 (1993) 141.
[23] R. Gopalan, Y.S. Lin, Ind. Eng. Chem. Res. 34 (1995) 1189.
[24] G. Boschloo, A. Hagfeldt, Chem. Phys. Lett. 370 (2003) 381.
[25] D.J. Bjorkert, R. Mayappan, D. Holland, M.H. Lewis, J. Eur. Ceram. Soc. 19 (1999) 1847.
[26] M.S.P. Francisco, V.R. Mastelaro, Chem. Mater. 14 (2002) 2514.
[27] C.P. Sibu, K.S. Rajesh, P. Mukundan, K.G.K. Warrier, Chem. Mater. 14 (2002) 2876.
[28] K.T. Ranjit, I. Willner, S.H. Bossmann, A.M. Braun, Environ. Sci. Technol. 35 (2001) 1544.
[29] J. Lin, J.C. Yu, J. Photochem. Photobiol. A: Chem. 116 (1998) 63.
[30] D.W. Hwang, J.S. Lee, W. Li, S.H. Oh, J. Phys. Chem. B 107 (2003) 4963.
[31] Y.H. Zhang, H.X. Zhang, Y.X. Xu, Y.G. Wang, J. Mater. Chem. 13 (2003) 2261.
[32] X.Z. Ding, X.H. Liu, J. Mater. Res. 13 (1998) 2556.
[33] (a) J.P. Shoffner, Anal. Chem. 47 (1975) 341;
(b) D.L. Rabenstein, Anal. Chem. 43 (1971) 1599.
[34] (a) T. Wu, G. Liu, J. Zhao, H. Hidaka, N. Serpone, J. Phys. Chem. B 102 (1998) 5845;
(b) C. Chen, W. Zhao, J. Li, J. Zhao, H. Hidaka, N. Serpone, Environ. Sci. Technol. 36 (2002) 3604.
[35] (a) T. Watanabe, T. Takizawa, K. Honda, J. Phys. Chem. 81 (1977) 1845;
(b) T. Inoue, T. Watanabe, A. Fujishima, K. Honda, K. Kohayakawa, J. Electrochem. Soc. 124 (1977) 719.